Chemical Science

EDGE ARTICLE

View Article Online
View Journal | View Issue

Cite this: *Chem. Sci.*, 2017, **8**, 3031

Acid/base triggered interconversion of μ-η²:η²-peroxido and bis(μ-oxido) dicopper intermediates capped by proton-responsive ligands†

V. E. Goswami,[a] A. Walli,[a] M. Förster,[b] S. Dechert,[a] S. Demeshko,[a] M. C. Holthausen*[b] and F. Meyer*[a]

Received 31st October 2016
Accepted 22nd January 2017

DOI: 10.1039/c6sc04820j

rsc.li/chemical-science

$Cu_2^{II}(\mu\text{-}\eta^2\text{:}\eta^2\text{-peroxido})$ and $Cu_2^{III}(\mu\text{-oxido})_2$ cores represent key intermediates in copper/dioxygen chemistry, and they are mechanistically important for biological hydroxylation and oxidation reactions mediated by dinuclear (type III) copper metalloenzymes. While the exact nature of the active species in different enzymes is still under debate, shifting equilibria between Cu_x/O_2 species is increasingly recognized as a means of switching between distinct reactivity patterns of these intermediates. Herein we report comprehensive spectroscopic, crystallographic and computational analysis of a family of synthetic $Cu_2^{II}(\mu\text{-}\eta^2\text{:}\eta^2\text{-peroxido})$ and $Cu_2^{III}(\mu\text{-oxido})_2$ dicopper complexes with a bis(oxazoline) (BOX) capping ligand. In particular, we demonstrate that a reversible peroxido/bis(μ-oxido) interconversion of the $[Cu_2O_2]$ core can be triggered by peripheral (de)protonation events on the ligand backbone. As the copper ions in the enzymes are typically supported by histidine imidazoles that offer a backside N atom amenable to potential (de)protonation, it is well conceivable that the shifting of equilibria between the $[Cu_2O_2]$ species in response to changes in local pH is biologically relevant.

Introduction

Dioxygen binding to copper in the active sites of metalloproteins has received much attention in past decades.[1] These metalloenzymes serve as prototypes for the development of bioinspired catalysts that can mediate the selective oxidation and oxygenation of C–H bonds, which is increasingly relevant for viable fuel and chemical feedstock formation.[2] Major research efforts in bioinorganic chemistry have been devoted to the development of small model complexes that mimic various aspects of the structure and function of the natural enzymes.[3–8] Owing to their specific design, it is often possible to trap key intermediates in such systems and to characterize their intrinsic reactivities in much greater detail than for the metalloenzymes themselves. The ultimate challenge is to understand the origin of the remarkable selectivity of the biochemical role models and to exploit the same concepts for the development of efficient synthetic catalysts.[2,9]

A variety of Cu_x/O_2 intermediates with different dioxygen binding modes have been uncovered and their diagnostic spectroscopic features and distinct reactivities are reasonably well understood.[1–3,6,7,10] Binuclear complexes with a $\mu\text{-}\eta^2\text{:}\eta^2$ peroxido dicopper(II) core (**P** in Scheme 1), as found in oxy-haemocyanin or oxy-tyrosinase, are among the most prominent species, and synthetically useful biomimetic analogs capable of hydroxylating exogenous phenol substrates are starting to emerge.[11–14] In model studies, it has been shown that dicopper complexes bearing a bis(μ-oxido) dicopper(III) core (**O**) are capable of C–H bond hydroxylation as well.[15–18] In solution, the thermodynamic preference for the **P** or the **O** core depends on

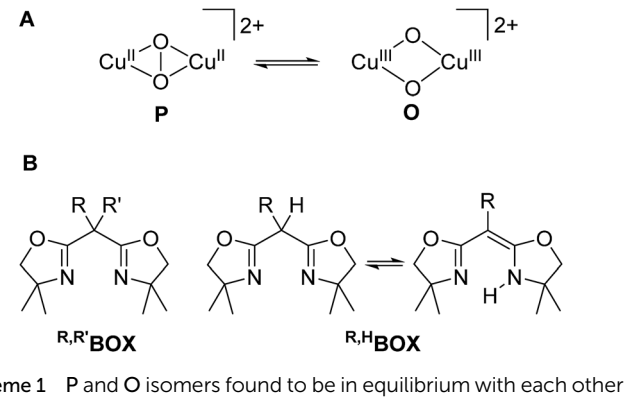

Scheme 1 P and O isomers found to be in equilibrium with each other (A). Bis-oxazoline(BOX) ligands used in this work (B).

[a]*Institut für Anorganische Chemie, Georg-August-Universität Göttingen, Tammannstraße 4, 37077 Göttingen, Germany. E-mail: franc.meyer@chemie.uni-goettingen.de*

[b]*Institut für Anorganische und Analytische Chemie, Goethe-Universität Frankfurt, Max-von-Laue-Straße 7, 60438 Frankfurt am Main, Germany. E-mail: max.holthausen@chemie.uni-frankfurt.de*

† Electronic supplementary information (ESI) available. CCDC 1511427–1511431. For ESI and crystallographic data in CIF or other electronic format see DOI: 10.1039/c6sc04820j

the subtle influence of the particular supporting ligand, the solvent and the nature of counterions, and in some cases both isomers have been reported to coexist in rapid equilibrium.[15,19–22] These findings have spurred vivid discussions regarding the nature of the active species in hydroxylation reactions[13,23–28] and the **P**/**O** core interconversion is increasingly recognized as being mechanistically relevant. Herein we report on an unprecedented pH-dependent **P**/**O** interconversion reaction, triggered by (de) protonation events in a bioinorganic model complex, which appears to be of particular relevance for such reactions in biological systems.

Results and discussion

We have recently shown that bidentate bis(oxazoline)s (BOXs), which are easily accessible and represent a privileged ligand class, are well-suited for supporting biomimetic Cu/O_2 chemistry.[29] By spectroscopic means we demonstrated that several ligands, ^{R,H}BOXs (Scheme 1B), reversibly bind to dioxygen to form μ-η^2:η^2-peroxidodicopper(II) complexes, both in solution and in the solid state; the thermodynamic and kinetic parameters of the **P** core formation have been determined.[29] Furthermore, we have shown that certain free bis(oxazoline)s, ^{R,H}BOXs, exist as an equilibrium mixture between the diimine and iminoenamine tautomers.[30] The latter are reminiscent of β-diketimines used extensively as anionic ligands after deprotonation, which led us to consider ^{R,H}BOXs as proton responsive ligands. We have now exploited this concept in bioinspired Cu/O_2 chemistry to study an acid/base triggered interconversion between the **P** and **O** cores.

Reactions of $^{R,R'}$BOX with $[Cu(MeCN)_4]ClO_4$ in tetrahydrofuran (THF) gave the air sensitive copper(I) complexes [($^{R,R'}$BOX)Cu(MeCN)]ClO_4, **1** (R = R′ = Me), **2** (R = Me, R′ = H), **3** (R = R′ = H)[29] as colourless compounds (see ESI†). Oxygenation of **1**, **2** and **3** in THF at 193 K led to deep purple coloured solutions of $[\{^{R,R'}BOX(THF)Cu\}_2(\mu\text{-}\eta^2\text{:}\eta^2\text{-}O_2)](ClO_4)_2$, ^{P}**4** (R = R′ = Me), ^{P}**5** (R = Me, R′ = H) and ^{P}**6** (R = R′ = H) with intense optical features around 330 nm ($\varepsilon \approx 20 \times 10^3$ M^{-1} cm^{-1}) and 500 nm ($\varepsilon \approx 1 \times 10^3$ M^{-1} cm^{-1}). For a detailed assignment we performed time-dependent density functional theory (TD-DFT) calculations on the μ-η^2:η^2 peroxido complex ^{P}**5**, including a coordinating ClO_4^- anion in the simulations.[31] In good agreement with experiment, the simulated spectrum for ^{P}**5** shows an intense absorption at 340 nm and a shallow band around 535 nm (Fig. 1b, see ESI† for a detailed discussion). The former absorption originates from a σ → σ* intra-core charge transfer (*i.e.*, from an occupied in-plane $d_{xy}(Cu^{II})/\pi^*(O_2^{2-})/d_{xy}(Cu^{II})$ bonding orbital combination into its antibonding counterpart), typically observed for μ-η^2:η^2 peroxido complexes.[26,29,32] The shallow absorption band at 535 nm is assigned to an intra-core π* → σ* transition (*i.e.*, from the out-of-plane π* of the O_2^{2-} ligand into the in-plane $d_{xy}(Cu^{II})/\pi^*(O_2^{2-})/d_{xy}(Cu^{II})$ antibonding orbital combination).

Single crystals of ^{P}**4** and ^{P}**5** were grown by Et_2O diffusion into THF : acetone (1 : 1) solutions at 193 K. X-ray diffraction analysis revealed the centrosymmetric molecular structures of the dications (^{P}**4** and ^{P}**5**) as shown in Fig. S11† and Fig. 2. Each copper ion is found in a slightly distorted square pyramidal (SP-5) coordination environment (τ = 0.16 in ^{P}**4**, 0.14 in ^{P}**5**) consisting of the respective BOX capping ligand, the bridging side-on μ-η^2:η^2 peroxide (d_{Cu-O} = 1.92–1.93 Å) and a THF solvent molecule bound in the apical position (d^{THF}_{Cu-O} = 2.32/2.33 Å).

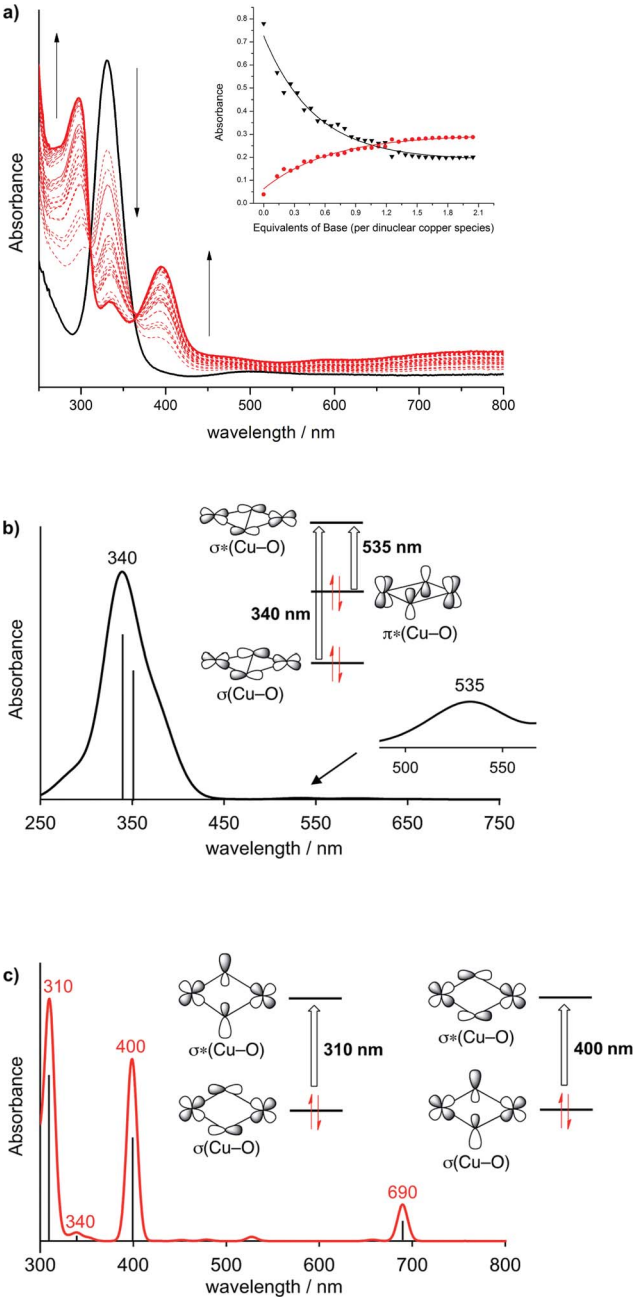

Fig. 1 (a) UV-vis monitoring of the titration of ^{P}**5** with DBU to give ^{O}**7**. The inset shows the decrease of the band at 333 nm (black triangles) and the rise of the new band at 395 nm (red circles) depending on the equivalents of DBU added. Simulated UV-vis spectra and simplified assignments of electronic transitions ignoring ligand contributions for (b) the dicationic peroxido complex ^{P}**5** (FWHM = 40) and (c) the neutral bis(μ-oxido) complex ^{O}**7**, calculated at the BLYP-D3/def2-TZVP(SDD)/COSMO(THF) level (FWHM = 13).

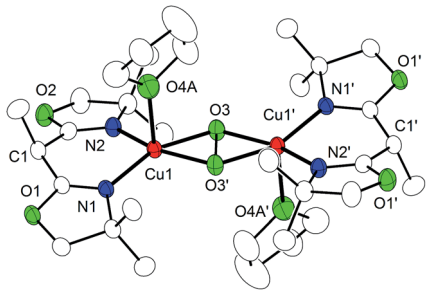

Fig. 2 Molecular structure of the cationic part of ^{P}5; 30% probability ellipsoids. Hydrogen atoms have been omitted for clarity.

While the Cu···Cu separations of 3.52 Å (^{P}4) or 3.50 av. Å (^{P}5) are typical for **P** cores, the bridging peroxido ligands exhibit the largest bond lengths (^{P}4: 1.56 Å, ^{P}5: 1.58 Å) reported so far for synthetic and biological Cu(μ-η^2:η^2-O$_2$)Cu systems (Table S3† presents a compilation of geometric and spectroscopic features of all literature-known μ-η^2:η^2-peroxidodicopper(II) species).[33–38] Most of the metric parameters of ^{P}4 and ^{P}5 are in excellent agreement with those derived from Cu K-edge extended X-ray absorption fine structure (EXAFS) data, for the corresponding **P** cores obtained with the capping ligands ^{tBu,H}BOX (^{tBu,H}**P**) and ^{H,H}BOX (^{H,H}**P**).[29]

Resonance Raman (rR) spectroscopy (λ_{ex} = 633 nm) of a THF solution of ^{P}4 at 193 K (Fig. 3) and frozen THF solutions of ^{P}5 and ^{P}6 at 77 K showed an oxygen isotope sensitive feature around 740 cm^{-1} which shifts to around 700 cm^{-1} when using ^{18}O$_2$ (^{P}4: 744 cm^{-1}, Δ[^{18}O$_2$] = −40 cm^{-1}; ^{P}5: 735 cm^{-1}, Δ[^{18}O$_2$] = −39 cm^{-1}; ^{P}6:[29] 742 cm^{-1}, Δ[^{18}O$_2$] = −39 cm^{-1}). These values fall in the typical range reported for O–O stretching vibrations of **P** cores (730−760 cm^{-1} with Δ[^{18}O$_2$] of *ca.* −40 cm^{-1},[1,39] including oxy-hemocyanin[40] and oxy-tyrosinase[41]). Obviously, the exceptionally long O–O bonds found in ^{P}4 and ^{P}5 do not translate into unusual rR signatures.[42,43]

Experimental data for the magnetic coupling in Cu$_2$/O$_2$ systems determined by SQUID magnetometry are still scarce, mostly because of the thermal lability of such intermediates. Magnetic susceptibility measurements for crystalline material of ^{P}4 confirmed the common S = 0 ground state resulting from very strong antiferromagnetic coupling between the cupric ions.[44,45]

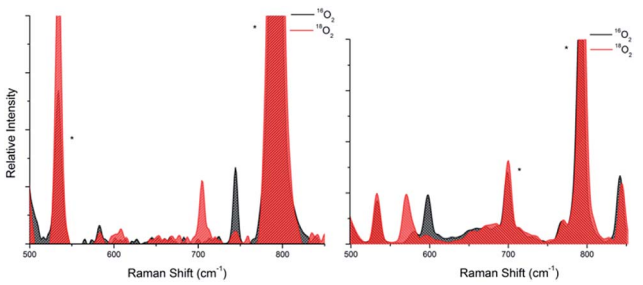

Fig. 3 Resonance Raman spectrum of ^{P}4 (left) in THF and ^{O}7 (right) in THF/pentane (1 : 1) at 193 K. The ^{16}O$_2$ spectra are in black and the ^{18}O$_2$ spectra are in red. Residual solvent signals are marked with an asterisk (*).

Simulations showed that the lower limit of the exchange coupling is very high, $-J \geq 800$ cm^{-1}, based on $H = -2JS_1S_2$ (Fig. S3†).[46] This is similar to the singlet–triplet splitting observed for oxy-hemocyanin ($-J \geq 300$ cm^{-1})[47] and some Cu(μ-η^2:η^2-O$_2$) Cu model systems.[48,49] In summary, the cationic cores of ^{P}4–^{P}6 represent genuine Cu(μ-η^2:η^2-O$_2$)Cu species with all their characteristic structural, spectroscopic and magnetic signatures, though with unusually long O–O bonds. Optical features of these complexes are essentially identical when recorded in THF or in a 1 : 1 THF : acetone solution, confirming the integrity of the **P** cores.

Titration of the purple coloured solutions of ^{P}5 or ^{P}6 in THF with the base diazabicycloundecane (DBU) at low temperatures (193 K) caused a distinct colour change to dark green. Spectral changes were monitored by *in situ* UV-vis spectroscopy and showed the gradual fading of the bands typical for the **P** core with the concomitant rise of new bands at 297 nm and 395 nm (Fig. 1a). Full conversion was reached after the addition of about 2 equivalents of DBU per dinuclear copper species, and the resulting products ^{O}7 and ^{O}8 seemed reasonably stable in the presence of excess DBU. Interestingly, ^{O}7 could also be prepared directly from the deprotonated ligand [^{Me}BOX]$^-$, which was obtained as an air sensitive white powder by treating ^{Me,H}BOX with one equivalent of *n*BuLi (see ESI† for details). Reaction of [^{Me}BOX]$^-$ with [Cu(MeCN)$_4$]ClO$_4$ in THF gave an air sensitive yellow colored solution of the complex [(^{Me}BOX)Cu^{I}] (characterized by NMR spectroscopy and ESI-MS; see ESI†). Subsequent oxygenation in THF at 193 K yielded a dark green coloured solution with optical features identical to those resulting from the titration experiment starting from ^{P}5. This corroborates that DBU serves as a base to abstract the backbone protons of the ^{Me,H}BOX capping ligands in ^{P}5 (Scheme 2).

In THF solution, ^{O}7 and ^{O}8 both feature three dominant absorption bands with λ_{max}/nm (ε/M^{-1} cm^{-1}) around 300 (~2.6 × 10^4), 335 (~7–8 × 10^3) and 400 (~10–11 × 10^3) typical for bis(μ-oxido) dicopper(III) species.[50,51] This suggests that peripheral deprotonation of the terminal ^{Me,H}BOX ligand in ^{P}5 and

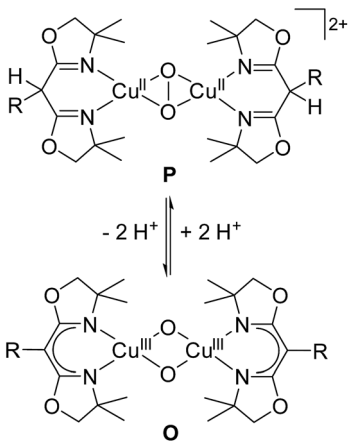

Scheme 2 Acid/base mediated interconversion between the **P** core of ^{P}5 (R = Me) and ^{P}6 (R = H) and the **O** core of ^{O}7 (R = Me) and ^{O}8 (R = H).

^{H,H}BOX ligand in ^{P}**6** triggers conversion of the ^{R,H}**P** to the ^{R}**O** core (Scheme 2). The simulated spectrum of ^{O}**7** obtained from TD-DFT calculations shows four absorption bands at 310, 340, 400 and 690 nm, which is in pleasant agreement with the experimental spectrum (for a simplified assignment of the two dominant transitions see Fig. 1c, for details the ESI†). Similar optical features have been observed by Herres-Pawlis *et al.* for a guanidine supported bis(μ-oxido) complex, and these authors arrived at an identical assignment of the electronic transitions underlying the two dominant absorptions.[52] The band at 690 nm originates from a ligand-to-metal charge transfer with BOX-centered donor MO (*cf.* the ESI†).

rR spectroscopy of a solution of ^{O}**7** at 193 K in a 1 : 1 mixture of THF and pentane revealed a single oxygen isotope sensitive feature at 598 cm^{-1} ($\Delta[^{18}O] = -26$ cm^{-1}) typical for the breathing mode of the **O** core (Fig. 3, right). Final proof came from X-ray diffraction analysis of the single crystals of ^{O}**7**, grown by slow diffusion of Et_2O into a 1 : 1 ^{Me}THF : pentane solution at 193 K. ^{O}**7** has a molecular structure with crystallographically imposed C_2 symmetry, each copper ion being ligated by one bidentate $[^{Me}BOX]^-$ ligand and the two bridging oxo atoms. The copper coordination geometry is significantly distorted from square planar (angle between the OCuO and NCuN planes: 24.5°) because the terminal $[^{Me}BOX]^-$ ligands are severely twisted with respect to each other (Fig. 4). In line with expectation, the Cu–N and Cu–O bonds (1.91 Å and 1.82 Å, respectively) are significantly shorter than in ^{P}**4** and ^{P}**5**. The Cu···Cu distance contracts to 2.87 Å, and the O···O separation of 2.24 Å evidences cleavage of the O–O bond. The combined data clearly indicate that ^{O}**7** is indeed $[(^{Me}BOXCu)_2(\mu\text{-}O)_2]$, an unusual example of a neutral bis(μ-oxido) dicopper(III) complex.[53,54]

Deprotonation and transformation of the **P** into the **O** core also leads to some notable changes in the ligand backbone. Angles around the bridging carbon atoms (C1) change from 109.2(4)°–114.9(4)° in ^{P}**5** (in one of the two crystallographically independent cations, the second one is disordered) to 118.6(4)°–120.8(4)° in ^{O}**7**. The sp^2 character of this carbon atom is also reflected in the bond lengths (excluding C–CH_3) which are approximately 0.1 Å shorter in ^{O}**7**. Furthermore C1 is now located within the plane of its three surrounding carbon atoms (0.02 Å deviation *vs.* 0.45 Å in the case of ^{P}**5**).

A DFT assessment of the **P**/**O** core isomerization for ^{P}**5** and ^{O}**7** nicely corroborates the experimental observations (Scheme 3): for ^{P}**5**, the peroxido isomer is found to be more stable than the bis(μ-oxido) isomer ^{O}**5** by $\Delta G^{193} = 4$ kcal mol^{-1}, and is separated from the latter by a barrier of $\Delta^{\ddagger}G^{193} = 10$ kcal mol^{-1}. For the neutral complex ^{O}**7**, a reverse stability order results with ^{O}**7** being favored by 7 kcal mol^{-1} over ^{P}**7**, and an interconversion barrier of 11 kcal mol^{-1} was computed. Moreover, the computational results indicate that a putative singly (de)protonated species (for which we find the bis(μ-oxido) isomer to be more stable, ESI†) should not be present in solution as it is thermodynamically disfavored against decomposition into ^{P}**5** and ^{O}**7**.

Addition of common Brönstedt acids ([LuH]OTf, $[LuH]BF_4$ and $HBF_4 \cdot Et_2O$ where LuH = lutidinium) to solutions of ^{O}**7** at 193 K did not trigger back-isomerization to the μ-η^2:η^2-peroxido species ^{P}**5**, but led to decomposition instead. However, the reversibility of the equilibrium shown in Scheme 2 was demonstrated by the following experiment: reaction of two equivalents of ^{H,H}BOX with one equivalent of $[Cu(MeCN)_4]ClO_4$ in THF in the presence of O_2 directly led to the formation of the bis(μ-oxido) complex ^{O}**8**. In this case, deprotonation is accomplished by excess ^{H,H}BOX acting as a Brönstedt base.[55] Similarly, *in situ* UV-vis monitoring of ^{H,H}BOX titration into a solution of ^{P}**6** (**P** core) indicated the formation of ^{O}**8** (**O** core) (Fig. 5 and S7†). Subsequent titration of $[Cu(MeCN)_4]ClO_4$ into the reaction mixture in the presence of excess O_2, in turn, resulted in the

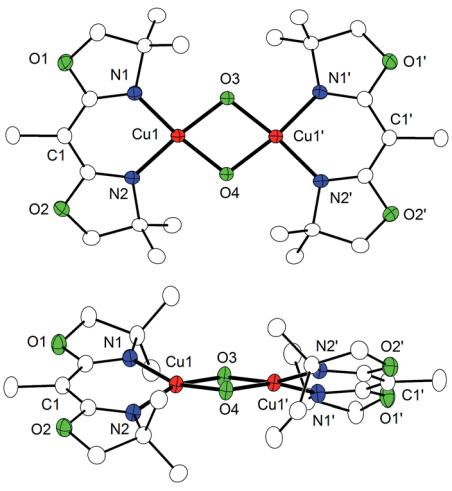

Fig. 4 Molecular structure of ^{O}**7** (top view and side view) with 30% probability ellipsoids. Hydrogen atoms and solvent molecules have been omitted for clarity.

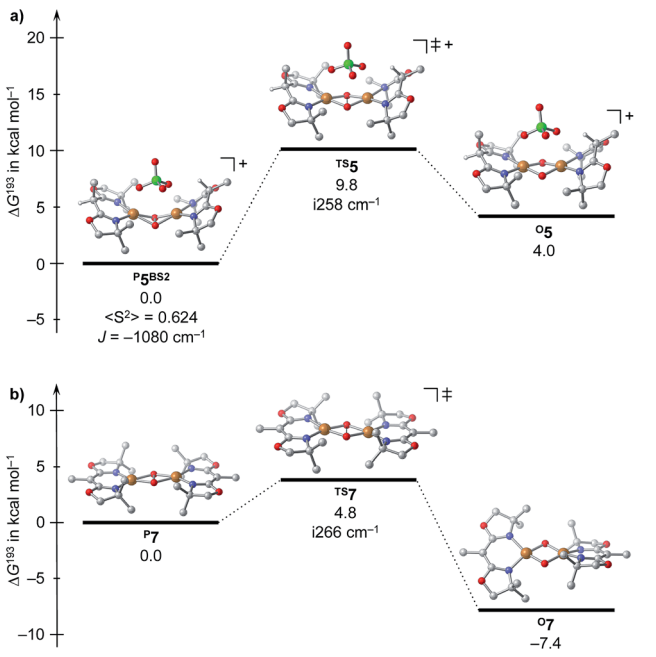

Scheme 3 Isomerization reactions for ^{P}**5**^{BS2} (a) and ^{P}**7** (b) computed at the BLYP-D3/def2TZVP(SDD)/COSMO(THF)//PBE-D3/def2TZVP(SDD)/SMD(THF) level of DFT.

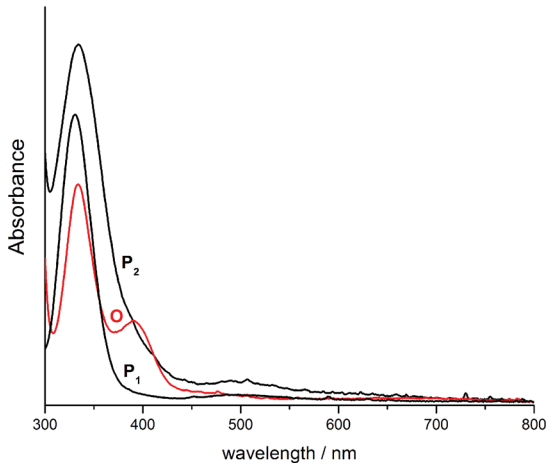

Fig. 5 UV-vis monitoring of the reaction sequence demonstrating the interconversion of ^{P}**6** to ^{O}**8** using ^{H,H}BOX as a base and subsequent conversion of ^{O}**8** back to ^{P}**6** upon addition of $[Cu(MeCN)_4]ClO_4$ in the presence of O_2 (baseline correction and dilution factor applied).

conversion back to ^{P}**6** (Fig. 5 and S8†). Thus, re-protonation of the ligand backbone in ^{O}**8** is accomplished by $[H^{H,H}BOX]^+$. This procedure enables complete control of the **P**/**O** interconversion without the need of adding exogenous acids. UV-vis monitoring of the reaction sequence (Fig. 5) confirmed that close to 1 equivalent of ^{O}**8** is formed during the first step, and a further 0.25 equivalents of ^{P}**6** result after addition of the second equivalent of $[Cu(MeCN)_4]ClO_4$ (Fig. 5).[56]

On warming from 193 K to room temperature, the intensely colored solutions of ^{P}**4**, ^{P}**5**, and ^{O}**7** gradually changed to light blue, indicating decay of the dicopper/dioxygen complexes. IR spectra of the light blue solid material isolated thereafter showed a characteristic OH stretching vibration around 3480 cm^{-1} (Fig. S4†). Single crystals of the material were obtained employing Cu(I) triflate as the metal source, and X-ray crystallography revealed the formation of the dihydroxido complex $[(^{Me,Me}BOXCu)_2(\mu\text{-}OH)_2](CF_3SO_3)_2$ (**9**, Cu···Cu separation: 3.00 Å) (Fig. 6). No degradation or oxygenation of the BOX ligands was observed.

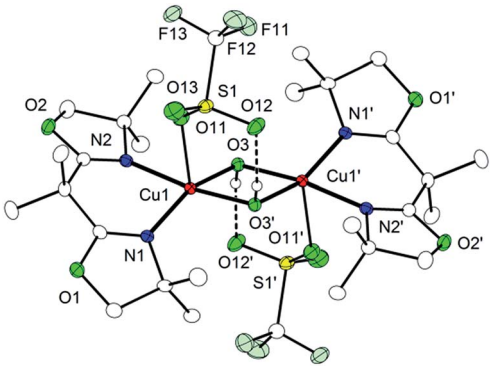

Fig. 6 Molecular structure of **9** set at 30% probability. Most hydrogen atoms have been omitted for clarity.

Conclusions

In conclusion, we have shown that the peroxido/bis(μ-oxido) interconversion in a $[Cu_2O_2]$ complex supported by proton-responsive BOX ligands can be controlled by peripheral (de) protonation events on the ligand backbone. We suggest this system as a bioinorganic mimic for type III dicopper proteins (or the dicopper active site of pMMO) in which the Cu ions are supported by histidine imidazoles, which offer a backside N atom amenable to potential (de)protonation equilibria in response to changes in local pH. In fact, (de)protonation of histidine imidazole ligands in metalloproteins is widely used for tuning redox potentials and electronic structures of the metallocofactors,[57–60] and it is an integral part of biologically important proton coupled electron transfer (PCET) reactivity (such as in the Rieske proteins).[61] It is an interesting perspective to introduce, *via* proton-responsive ligands, PCET reactivity to Cu_x/O_2 intermediates. We are currently pursuing further studies in this direction.

Acknowledgements

Financial support by the DAAD (PhD fellowship for V. E. G.) and the DFG (IRTG 1422 Metals Sites in Biomolecules: Structures, Regulation and Mechanisms) is gratefully acknowledged. Quantum chemical calculations have been performed at the Center of Scientific Computing (CSC) Frankfurt on the FUCHS and LOEWE-CSC high-performance compute clusters.

Notes and references

1 E. I. Solomon, D. E. Heppner, E. M. Johnston, J. W. Ginsbach, J. Cirera, M. F. Qayyum, M. T. Kieber-Emmons, C. H. Kjaergaard, R. G. Hadt and L. Tian, *Chem. Rev.*, 2014, **114**, 3659.
2 J. Y. Lee and K. D. Karlin, *Curr. Opin. Chem. Biol.*, 2015, **25**, 184.
3 E. A. Lewis and W. B. Tolman, *Chem. Rev.*, 2004, **104**, 1047.
4 S. Itoh and S. Fukuzumi, *Acc. Chem. Res.*, 2007, **40**, 592.
5 L. Q. Hatcher and K. D. Karlin, *J. Biol. Inorg Chem.*, 2004, **9**, 669.
6 C. Citek, S. Herres-Pawlis and T. D. P. Stack, *Acc. Chem. Res.*, 2015, **48**, 2424.
7 L. M. Mirica, X. Ottenwaelder and T. D. P. Stack, *Chem. Rev.*, 2004, **104**, 1013.
8 S. Schindler, *Eur. J. Inorg. Chem.*, 2000, 2311.
9 M. Rolff, J. Schottenheim and F. Tuczek, *Chem. Soc. Rev.*, 2011, **40**, 4077.
10 E. I. Solomon, *Inorg. Chem.*, 2016, **55**, 6364.
11 A. Hoffmann, C. Citek, S. Binder, A. Goos, M. Rübhausen, E. C. Wasinger, T. D. P. Stack, O. Troeppner, I. Ivanovic and S. Herres-Pawlis, *Angew. Chem., Int. Ed.*, 2013, **52**, 5398.
12 J. Schottenheim, C. Gernert, B. Herzigkeit, J. Krahmer and F. Tuczek, *Eur. J. Inorg. Chem.*, 2015, 3501.
13 J. N. Hamann and F. Tuczek, *Chem. Commun.*, 2014, **50**, 2298.
14 J. N. Hamann, B. Herzigkeit, R. Jurgeleit and F. Tuczek, *Coord. Chem. Rev.*, 2017, **334**, 54.

15 J. A. Halfen, S. Mahapatra, E. C. Wilkinson, S. Kaderli, V. G. Young, L. Que, A. D. Zuberbühler and W. B. Tolman, *Science*, 1996, **271**, 1397.
16 S. Itoh, M. Taki, H. Nakao, P. L. Holland, W. B. Tolman, L. Que Jr and S. Fukuzumi, *Angew. Chem., Int. Ed.*, 2000, **39**, 398.
17 J. B. Gary, C. Citek, T. A. Brown, R. N. Zare, E. C. Wasinger and T. D. P. Stack, *J. Am. Chem. Soc.*, 2016, **138**, 9986.
18 J. Becker, P. Gupta, F. Angersbach, F. Tuczek, C. Naether, M. C. Holthausen and S. Schindler, *Chem. – Eur. J.*, 2015, **21**, 11735.
19 H.-C. Liang, M. J. Henson, L. Q. Hatcher, M. A. Vance, C. X. Zhang, D. Lahti, S. Kaderli, R. D. Sommer, A. L. Rheingold, A. D. Zuberbühler, E. I. Solomon and K. D. Karlin, *Inorg. Chem.*, 2004, **43**, 4115.
20 X. Ottenwaelder, D. J. Rudd, M. C. Corbett, K. O. Hodgson, B. Hedman and T. D. P. Stack, *J. Am. Chem. Soc.*, 2006, **128**, 9268.
21 J. Cahoy, P. L. Holland and W. B. Tolman, *Inorg. Chem.*, 1999, **38**, 2161.
22 L. Q. Hatcher, M. A. Vance, A. A. Narducci Sarjeant, E. I. Solomon and K. D. Karlin, *Inorg. Chem.*, 2006, **45**, 3004.
23 S. Itoyama, K. Doitomi, T. Kamachi, Y. Shiota and K. Yoshizawa, *Inorg. Chem.*, 2016, **55**, 2771.
24 M. A. Culpepper, G. E. Cutsail, B. M. Hoffman and A. C. Rosenzweig, *J. Am. Chem. Soc.*, 2012, **134**, 7640.
25 C. Citek, J. B. Gary, E. C. Wasinger and T. D. P. Stack, *J. Am. Chem. Soc.*, 2015, **137**, 6991.
26 C. Wilfer, P. Liebhäuser, A. Hoffmann, H. Erdmann, O. Grossmann, L. Runtsch, E. Paffenholz, R. Schepper, R. Dick and S. Herres-Pawlis, *Chem. – Eur. J.*, 2015, **21**, 17639.
27 L. Chiang, W. Keown, C. Citek, E. C. Wasinger and T. D. P. Stack, *Angew. Chem., Int. Ed.*, 2016, **55**, 10453.
28 M. Rolff, J. Schottenheim and J. Tuczek, *J. Coord. Chem.*, 2010, **63**, 2383.
29 A. Walli, S. Dechert, M. Bauer, S. Demeshko and F. Meyer, *Eur. J. Inorg. Chem.*, 2014, 4660.
30 A. Walli, S. Dechert and F. Meyer, *Eur. J. Org. Chem.*, 2013, 7044.
31 Density functional calculations were performed at the RI-BLYP-D3/def2-TZVP(SDD)/COSMO(THF)//RI-PBE-D3/def2-TZVP(SDD)/SMD(THF) level. The accuracy of this approach has been established by comparison to explicitly correlated CCSD(T)-F12b/CBS(T/Q) benchmark results (see the ESI† for further details). A similarly favorable performance of the BLYP functional for related chemistry has been documented recently: P. Gupta, M. Diefenbach, M. C. Holthausen and M. Förster, *Chem. – Eur. J.*, 2017, **23**, 1427.
32 N. C. Eickman, R. S. Himmelwright and E. I. Solomont, *Proc. Natl. Acad. Sci. U. S. A.*, 1979, **76**, 2094.
33 G. Y. Park, M. F. Qayyum, J. Woertink, K. O. Hodgson, B. Hedman, A. Sarjeant, E. I. Solomon and K. D. Karlin, *J. Am. Chem. Soc.*, 2012, **2**, 8513.
34 B. M. Lam, J. A. Halfen, V. G. Young, J. R. Hagadorn, P. L. Holland, A. Lledós, L. Cucurull-Sánchez, J. J. Novoa, S. Alvarez and W. B. Tolman, *Inorg. Chem.*, 2000, **39**, 4059.
35 M. Kodera, K. Katayama, Y. Tachi, K. Kano, S. Hirota and S. Fujinami, *J. Am. Chem. Soc.*, 1999, **121**, 11006.
36 N. Kitajima, K. Fujisawa, Y. Moro-oka and K. Toriumi, *J. Am. Chem. Soc.*, 1989, **111**, 8975.
37 N. Kitajima, K. Fujisawa, C. Fujimoto, Y. Moro-oka, S. Hashimoto, T. Kitagawa, K. Toriumi, K. Tatsumi and A. Nakamura, *J. Am. Chem. Soc.*, 1992, **114**, 1277.
38 Y. Funahashi, T. Nishikawa, Y. Wasada-Tsutsui, Y. Kajita, S. Yamaguchi, H. Arii, T. Ozawa, K. Jitsukawa, T. Tosha, S. Hirota, T. Kitagawa and H. Masuda, *J. Am. Chem. Soc.*, 2008, **130**, 16444.
39 M. J. Henson, P. Mukherjee, D. E. Root, T. D. P. Stack and E. I. Solomon, *J. Am. Chem. Soc.*, 1999, **121**, 10332.
40 C. R. Andrew, H. Yeom, S. Valentine, B. G. Karlsson, N. Bonander, G. Van Pouderoyen, G. W. Canters, T. M. Loehr and J. Sanders-Loehr, *J. Am. Chem. Soc.*, 1994, **116**, 11489.
41 N. C. Eickman, E. I. Solomon, J. A. Larrabee, T. G. Spiro and K. Lerch, *J. Am. Chem. Soc.*, 1978, **100**, 6529.
42 Dependent on the particular choice of functional, basis set and relativistic approach, DFT optimized structures for the peroxido isomer show significant variations in the O–O bond length, overall underestimating the experimentally determined value by −0.13 to −0.24 Å. Consistently, the O–O stretching vibration is substantially overestimated by 80–355 cm^{-1} compared to experiment, again depending on the DFT approach chosen. As detailed in the ESI,† the strong method dependence goes back to a very shallow stretching potential along the O–O bond: for example, a relaxed scan of the O–O bond length in ^{P}**5** performed at the BP86/SVP level of DFT from R_{O-O} = 1.46 Å (optimized minimum structure) to 1.58 Å (experimental bond length) results in an energy increase of merely 2.2 kcal mol^{-1}. Harmonic O–O stretching frequencies, however, computed for these two points vary by an enormous 260 cm^{-1}. These findings, together with the fact that the neglect of crystal packing effects and vibrational anharmonicities further complicate comparison with experiment, forced us to conclude that a quantitative modeling of structural and vibrational characteristics of the peroxido species studied here is outside the scope of presently available density functional methods.
43 While having a small amount of the O isomer in the crystals (see E. Pidcock, S. DeBeer, H. V. Obias, B. Hedman, K. O. Hodgson, K. D. Karlin and E. I. Solomon, *J. Am. Chem. Soc.*, 1999, **121**, 1870) cannot be completely ruled out, this seems unlikely because (i) free refinement turned out to be unstable when trying to model an O–O disorder in the crystallographic structures; (ii) similar long O–O bonds are observed for both complexes, ^{P}**4** and ^{P}**5**, the latter lacking the ligand backbone proton required for deprotonation-induced transformation to the corresponding bis(μ-oxido) species; and (iii) the rR spectra of both solid materials do not show any isotope sensitive bands at ∼600 cm^{-1} that could be assigned to the **O** isomer.
44 K. E. Dalle, T. Gruene, S. Dechert, S. Demeshko and F. Meyer, *J. Am. Chem. Soc.*, 2014, **136**, 7428.

45 N. Kindermann, E. Bill, S. Dechert, S. Demeshko, E. J. Reijerse and F. Meyer, *Angew. Chem., Int. Ed.*, 2015, **54**, 1738.
46 In good agreement with this experimentally determined lower limit, a broken-symmetry DFT assessment of ^{P}**5** resulted in $-J = 1080\ cm^{-1}$ (see Scheme 3 and the ESI†).
47 E. I. Solomon, *Chem. Rev.*, 1992, **92**, 521.
48 K. D. Karlin, Z. Tyeklár, A. Farooq, R. R. Jacobson, E. Sinn, D. W. Lee, J. E. Bradshaw and L. J. Wilson, *Inorg. Chim. Acta*, 1991, **182**, 1.
49 M. J. Baldwin, D. E. Root, J. E. Pate, K. Fujisawa, N. Kitajima and E. I. Solomon, *J. Am. Chem. Soc.*, 1992, **114**, 10421.
50 P. L. Holland, C. J. Cramer, E. C. Wilkinson, S. Mahapatra, K. R. Rodgers, S. Itoh, M. Taki, S. Fukuzumi, L. Que Jr and W. B. Tolman, *J. Am. Chem. Soc.*, 2000, **122**, 792.
51 For ^{O}**8** the relative intensity of the bands around 335 and 400 nm is inverted.
52 S. Herres-Pawlis, P. Verma, R. Haase, P. Kang, C. T. Lyons, E. C. Wasinger, U. Floerke, G. Henkel and T. D. P. Stack, *J. Am. Chem. Soc.*, 2009, **131**, 1154.
53 D. J. E. Spencer, N. W. Aboelella, A. M. Reynolds, P. L. Holland and W. B. Tolman, *J. Am. Chem. Soc.*, 2002, **124**, 2108.
54 B. F. Straub, F. Rominger and P. Hofmann, *Chem. Commun.*, 2000, **3**, 1611.
55 S. Milione and V. Bertolasi, *Tetrahedron Lett.*, 2011, **52**, 3570–3574.
56 Some decomposition occurs, and hence the re-formation of ^{P}**6** is not quantitative.
57 N. Nakanishi, F. Takeuchi and M. Tsubaki, *J. Biochem.*, 2007, **142**, 553.
58 E. Fadda, N. Chakrabarti and R. Pomes, *J. Phys. Chem. B*, 2005, **109**, 22629.
59 Y. Lin and C. Lim, *J. Am. Chem. Soc.*, 2004, **126**, 2602.
60 J. J. Warren and J. M. Mayer, *Biochemistry*, 2015, **54**, 1863.
61 A. Albers, S. Demeshko, S. Dechert, C. T. Souma, J. M. Mayer and F. Meyer, *J. Am. Chem. Soc.*, 2014, **136**, 3946.